Proc. VIII World Congress on the Theroy of Machines and Mechanisms,
Prague, Czechoslavakia, July 1991- Revised 10/1/90

THE DYNAMIC ANALYSIS OF FLEXIBILITY IN MOBILE ROBOTIC MANIPULATOR SYSTEMS

S. Dubowsky[1]
P.-Y. Gu[2]
J. F. Deck [3]

Department of Mechanical Engineering
Massachusetts Institute of Technology
Cambridge, MA 02139, USA

ABSTRACT

Robotic manipulators mounted on vehicles are being considered for a number of applications. Since the dynamic performance of these systems is affected by the flexibility of their manipulators' and vehicles' suspensions, analytical methods are required to model their dynamic behavior. This paper presents an effective method that models such a system's spatial dynamic behavior by considering the nonlinear dynamic characteristics which result from its manipulator's gross motions, accounts for spatial vibrations due to the distributed mass and flexibility of manipulator and vehicle, and includes the effects of the manipulator's and vehicle's control systems.

I. INTRODUCTION

Robotic systems are being considered for a wide variety of applications outside their traditional factory uses, such as in space, undersea, in nuclear contaminated environments and in medical hospitals [1-4]. Robots need to be mobile for these applications, consisting of manipulators carried by vehicles. Since these manipulators will be lightweight, they will have significant flexibility, particularly in space systems, which could affect system dynamic performance. Such performance may also be affected by vehicle characteristics like the suspension compliance of ground based vehicles.

Figure 1 shows two examples of ground based mobile manipulator systems. To design these systems and their control systems requires effective analytical methods able to model the dynamic behavior of flexible manipulators on flexible vehicles with compliant suspensions.

[1] Professor
[2] Graduate Research Assistant
[3] Graduate Research Assistant

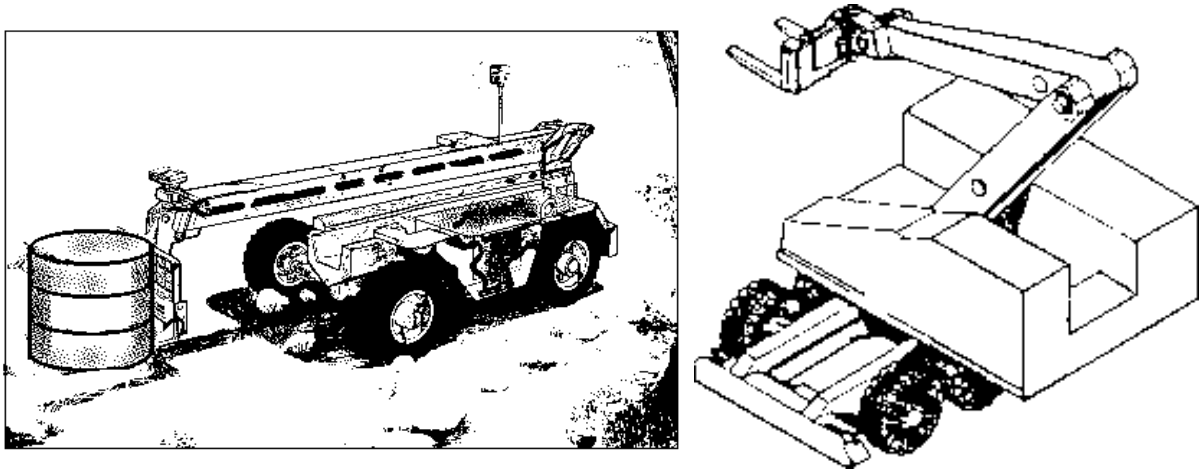

Figure 1. Examples of Mobile Manipulator Systems

The development of analytical models for fixed-base flexible machines and manipulators has been the subject of substantial research [5-9]. The studies of the control of flexible manipulators for space have not considered the dynamic interactions between the manipulator and its vehicle [10]. Some work has been done to construct dynamic models of rigid-link manipulators on moving vehicles; however past models to study the important dynamic interactions of a flexible manipulator on a flexible vehicle have been quite primitive [4,11,12].

Here a relatively general method is presented to model, in substantial detail, the fully spatial dynamic behavior of such a flexible system. This method extends the methodology presented in reference [5], considering the nonlinear dynamic characteristics of the system that result from the manipulator's gross time-varying spatial motions. It accounts for spatial vibrations due to the distributed mass and flexibility of the manipulator and vehicle, and the compliances of the vehicle's suspension, tires, and the ground. The method also includes the effects of the manipulator's and vehicle's control systems.

The technique combines Component Mode Synthesis (CMS) reduced finite element models of individual links and the vehicle with 4 by 4 Hartenberg-Denavit descriptions of the system's kinematic joints [5-6]. This allows the nonlinear dynamic equations of motion to be formulated for a system with realistically complex-shaped mechanical elements. CMS yields good computational efficiency without a serious loss of accuracy. The method can also represent control systems in highly general forms; vehicle's suspension characteristics can also be nonlinear and

quite general, as well. For example, this approach can incorporate complex tire / ground models for terrestrial systems.

Finally, the paper presents results for a typical system which show the importance of modeling the dynamic interactions that can exist between a manipulator, its flexibility, and its vehicle. The example shows that these interactions can result in significant degradation of the system's performance. For instance, manipulator motions that cause the vehicle to rock on its suspension lead to large errors in the position of the manipulator's end-effector. These errors can be compensated for by using a properly designed manipulator control system with end-point sensing, provided that the errors are not excessive and that stability problems are avoided, [13].

II. ANALYTICAL DEVELOPMENT OF MODELING TECHNIQUE

Hartenberg-Denavit 4 by 4 transformation matrices are used to represent the nominal motions of each body in the system, including the vehicle. The distributed mass and flexibility of these bodies are described using Finite Element Methods. The FE nodal displacement coordinates are called perturbation coordinates, and they describe the motions of the FE node points with respect to the nominal motion frame of each body. The dynamic equations of motion for each body are derived using Lagrange's formulation, in which the perturbation coordinates are the generalized coordinates. These equations are reduced by Component Mode Synthesis (CMS) to improve numerical efficiency. Compatibility matrices, which express the kinematic and force constraint relationships between the links, are used to assemble the dynamic equations of the system. The global dynamic equations of the system have the form:

$$[\mathbf{M}]\{\ddot{\mathbf{q}}\}+[\mathbf{G}]\{\dot{\mathbf{q}}\}+[\mathbf{K}]\{\mathbf{q}\}=\{\mathbf{Q}\} \qquad (1)$$

in which the matrices [**M**], [**G**] and [**K**] describe the mass, damping and stiffness characteristics of the system and, in general, are time varying. The vector {**q**}, and its derivatives $\{\dot{\mathbf{q}}\}$ and $\{\ddot{\mathbf{q}}\}$, are the global independent coordinates, velocities and accelerations. The vector {**Q**} describes the forces applied to the system, including actuator forces / torques and external loads. The matrices [**M**], [**G**], and [**K**], and the vector {**Q**}, are defined in terms of the links' finite element mass and stiffness matrices, $[\mathbf{M}_i^{FE}]$ and $[\mathbf{K}_i^{FE}]$; damping matrices that also include gyroscopic terms due to the nominal motions, $[\mathbf{G}_i]$; "gyroscopic stiffening" terms due to the nominal

motions, $[\tilde{\mathbf{K}}_i]$; the link's CMS transformation matrices, $[\mathbf{A}_i]$; the link compatibility matrices $[\mathbf{B}_i]$ and their derivatives; and derivatives of the link nominal motion joint variables, θ_i. They are given as follows:

$$[\mathbf{M}] = \sum_{i=1}^{NL} [\mathbf{B}_i]^T [\mathbf{A}_i]^T [\mathbf{M}_i^{FE}] [\mathbf{A}_i] [\mathbf{B}_i] \tag{2}$$

$$[\mathbf{G}] = \sum_{i=1}^{NL} \left\{ 2[\mathbf{B}_i]^T [\mathbf{A}_i]^T [\mathbf{M}_i^{FE}] [\mathbf{A}_i] \sum_{j=1}^{NL} \frac{\partial [\mathbf{B}_i]}{\partial \theta_j} \dot{\theta}_j + [\mathbf{B}_i]^T [\mathbf{A}_i]^T [\mathbf{G}_i] [\mathbf{A}_i] [\mathbf{B}_i] \right\} \ddot{y} \tag{3}$$

$$[\mathbf{K}] = \sum_{i=1}^{NL} [\mathbf{B}_i]^T [\mathbf{A}_i]^T [\mathbf{K}_i^{FE} + \tilde{\mathbf{K}}_i] [\mathbf{A}_i] [\mathbf{B}_i] + \sum_{i=1}^{NL} \sum_{j=1}^{NL} 2[\mathbf{B}_i]^T [\mathbf{A}_i]^T [\mathbf{G}_i] [\mathbf{A}_i] \frac{\partial [\mathbf{B}_i]}{\partial \theta_j} \dot{\theta}_j$$
$$+ \sum_{i=1}^{NL} \sum_{j=1}^{NL} \sum_{k=1}^{NL} [\mathbf{B}_i]^T [\mathbf{A}_i]^T [\mathbf{M}_i^{FE}] [\mathbf{A}_i] \left(\frac{\partial^2 [\mathbf{B}_i]}{\partial \theta_j \, \partial \theta_k} \dot{\theta}_j \, \dot{\theta}_k + \frac{\partial [\mathbf{B}_i]}{\partial \theta_j} \ddot{\theta}_j \right) \tag{4}$$

where NL is the number of links in the system. A computational block diagram of the technique is shown in Figure 2. The form of the compatibility matrices, $[\mathbf{B}_i]$, used to construct the equations of motion of the multibody system, is determined by the nature of the system's joints. These joints may be ideal, meaning that they apply kinematic constraints to the system, or they may be nonideal, with compliance and clearances [14].

III. SYSTEM DESCRIPTION

The analytical method briefly described above has been implemented in a software package called FLEXARM II. This program has been applied to several case studies of reasonably realistic systems, including mobile manipulators. Figure 3 shows a schematic diagram of such a system. For this paper, the manipulator is assumed to have three rigid-body degrees of freedom (DOF), defined by the joint angles θ_1, θ_2 and θ_3. The vehicle has six rigid-body degrees of freedom, consisting of three rotations, ψ_x, ψ_y and ψ_z, and three displacements, X, Y and Z. The angles ψ_x, ψ_y and ψ_z are rotations about the body-fixed vehicle axes **X**, **Y** and **Z**, shown in Figure 3. The displacements are parallel to the **X**, **Y** and **Z** axes.

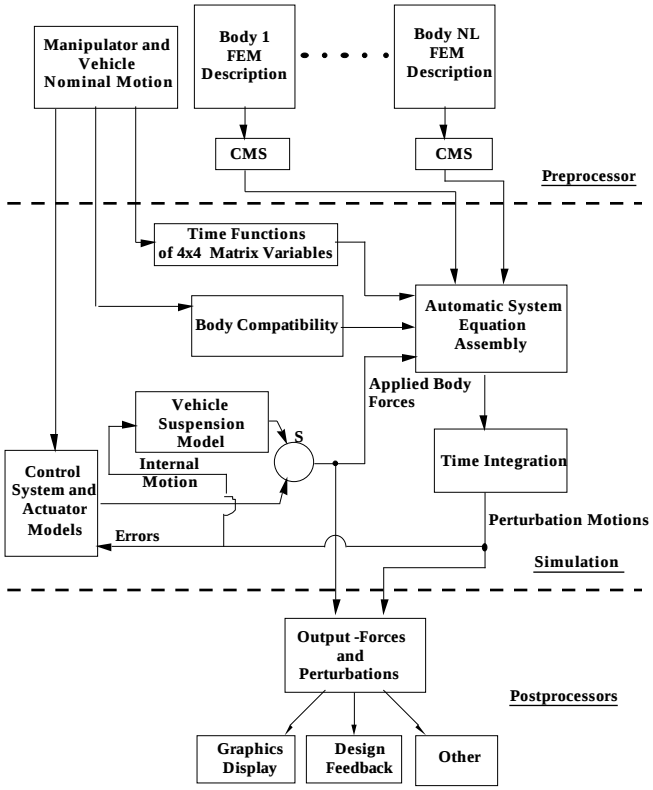

Figure 2. FLEXARM II Computational Block Diagram

The combined vehicle suspension and ground / tire compliance is represented by the linear stiffness and damping matrices. The elements of these matrices are chosen to give the rigid-body model, with its 25 kg payload, a natural frequency of 1.5 Hz in the **Z** direction and 10 Hz in the **X** and **Y** directions. The suspension damping is chosen to give the vehicle a damping ratio of 0.65 in all directions. The manipulator's joint control systems are simple linear PD controllers, each one with 10 Hz bandwidth and 0.707 damping ratio for the rigid body system. The control bandwidths are chosen to be approximately one third the lowest natural frequency of the flexible manipulator with its maximum 25 kg payload to avoid stability problems. These controllers include dynamic feedforward, using a simple fixed-base rigid manipulator model, to compensate for gravitational loads. Table 1 contains the important mass properties of the vehicle and manipulator.

Table 1. Mass Properties of Vehicle and Manipulator

	Mass (kg)	I_X (kg-m^2)	I_Y (kg-m^2)	I_Z (kg-m^2)
Vehicle	250.0	88.5	26.0	104.0
Link 1	7.4	1.6	0.2	1.6
Link 2	11.1	0.1	4.8	4.8
Link 3	11.1	0.2	4.7	4.7

Each of the manipulator's links is assumed to be constructed of a thin wall tube, with an outer diameter 0.2 m and an inner diameter 0.196 m, see Figure 4. The lengths of these links are 0.5 m, 0.75 m and 0.75 m, respectively, see Figure 5. The masses of the actuators are 20 kg for actuator 1, 50 kg for actuator 2, and 20 kg for actuator 3. The payload is assumed to be 25 kg.

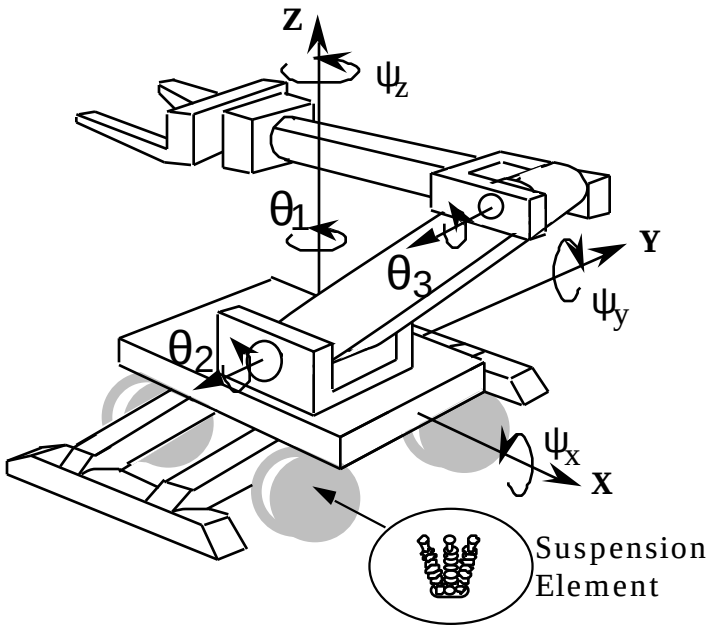

Figure 3. System Description

Finite element models are constructed for individual mechanical elements in the system, including the joints with their shafts, bearings, motors and encoders, such as shown in Figure 4, as required by the computational procedure shown in Figure 2. The flexible system model has twenty-three degrees of freedom after CMS reduction, including 6 degrees of freedom for the vehicle.

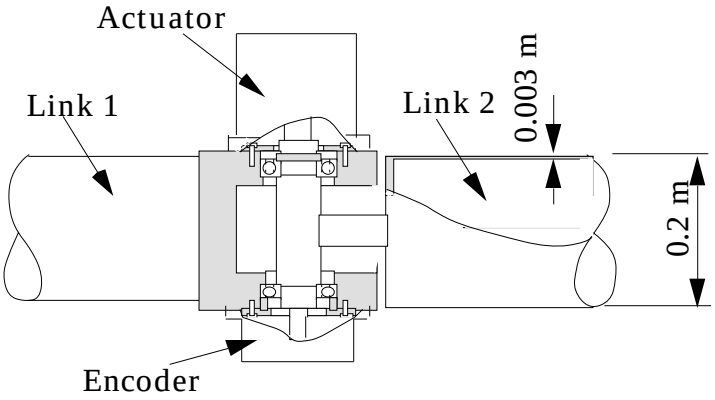

Figure 4. Model of Manipulator Joint 2

IV. RESULTS

For the results given in this paper, the manipulator is commanded to move its payload from initial position A to final position B, shown in Figure 5, in 2.5 seconds. The commanded joint angles for this motion are shown in Figure 6.

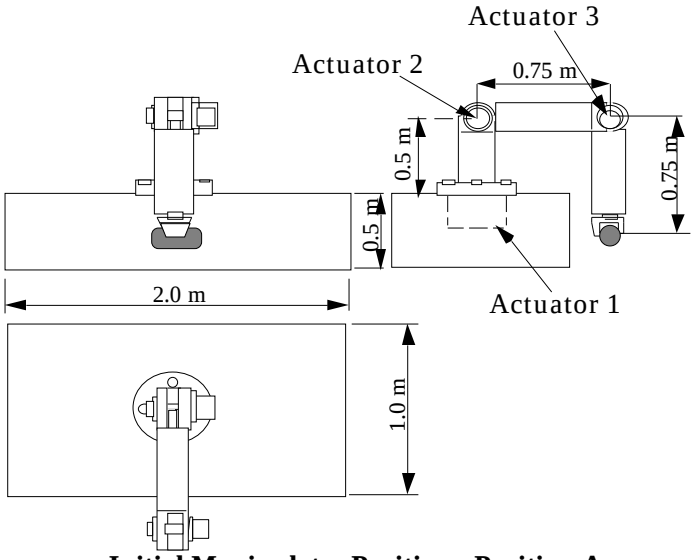

a. Initial Manipulator Position - Position A

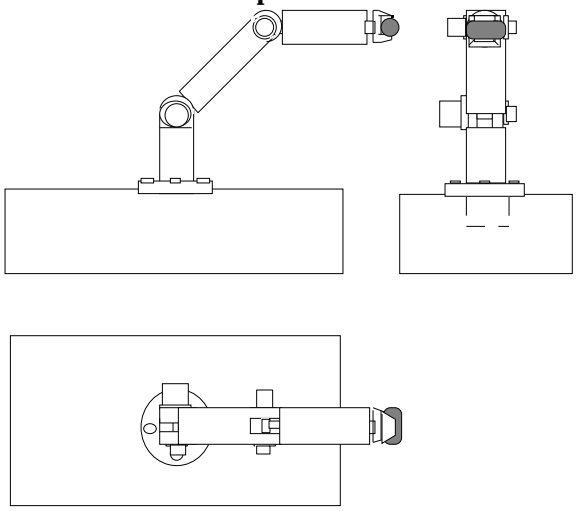

b. Final Manipulator Position - Position B

Figure 5. Initial and Final Manipulator Positions

When this motion is simulated by FLEXARM II with rigid manipulator links and the vehicle suspension locked, the manipulator has a maximum tip error of approximately 0.25 mm, as shown in Figure 7. This result includes the feedforward gravity compensator; hence this error represents the dynamic errors due to finite control system bandwidths. Without feedforward gravity compensation, the rigid manipulator's tip error increases to 3.5 mm. The actuator torques for this rigid link, locked suspension case are shown in Figure 8.

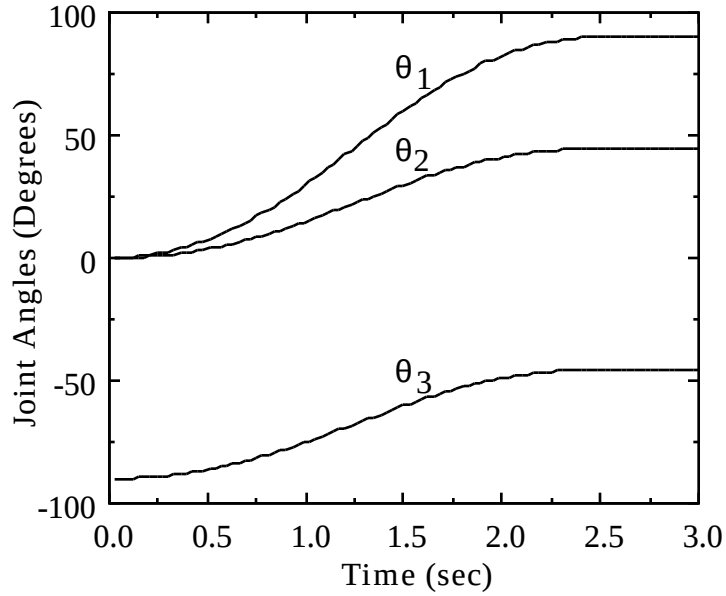

Figure 6. Commanded Joint Angles

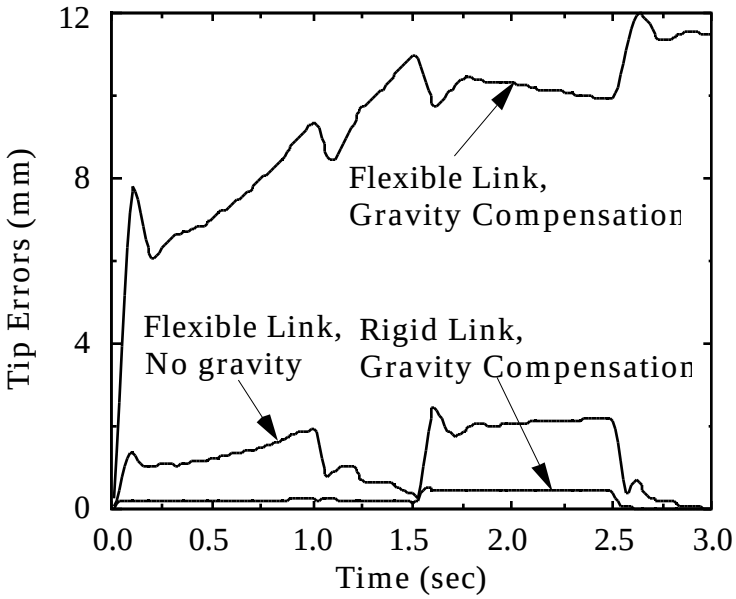

Figure 7. Tip Errors for Locked Suspension System - Rigid and Flexible Links

When link flexibility is included in the simulation, with no gravity, the maximum tip error increases to approximately 2.25 mm, see Figure 7. This error is due to the link flexing, excited by the dynamic forces. With gravity, and using a gravity compensator based on a rigid link manipulator model, the maximum tip error becomes 12 mm, 48 times greater than the error of the rigid link model, see Figure 7. The simple gravity compensation used can not offset the effects of the links bending under their own weight and the weight of the payload. This maximum tip error of 12 mm for the flexible link system may be unacceptable for some applications.

However, end-point control could be used to achieve precise positioning of the end-effector [13]. Figure 9 shows the joint actuator torques for the flexible links, locked vehicle suspension case. These torques are not substantially different from those of the rigid link case shown in Figure 8. Their slightly more oscillatory behavior is due to the flexibility of the joint and link structures.

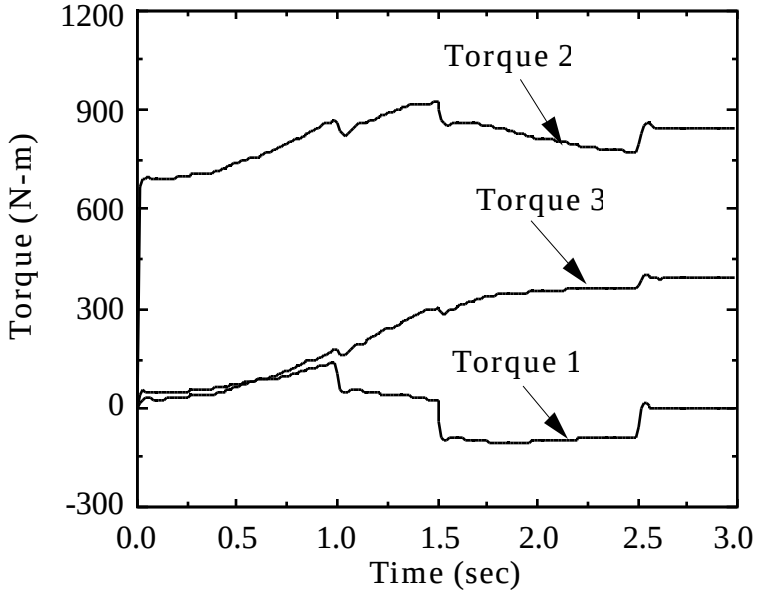

Figure 8. Joint Torques - Rigid links, Locked Suspension System

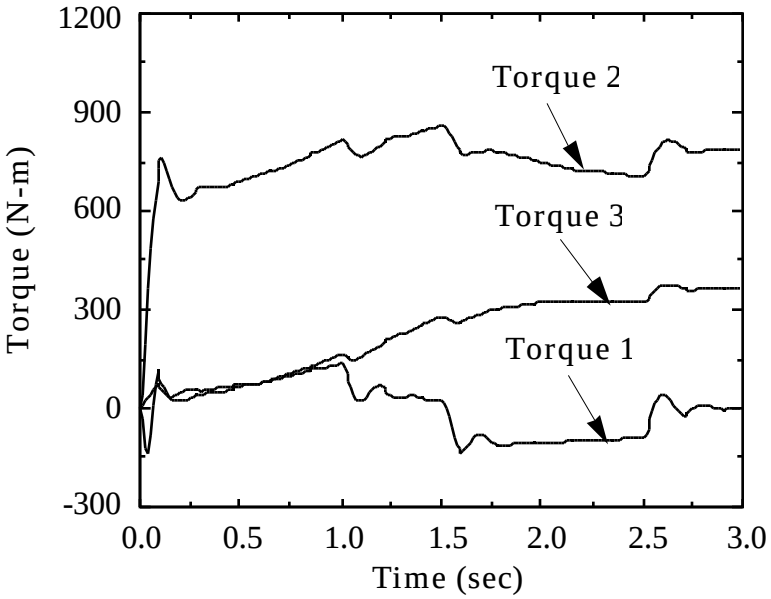

Figure 9. Joint Torques - Flexible Links, Locked Suspension System

When the compliance of the vehicle's suspension is included in the flexible manipulator simulation, the maximum tip error increases to nearly 250 mm, see Figure 10. The tip error for the flexible link manipulator on a locked suspension,

from Figure 7, is repeated in Figure 10. Comparing these two results shows that the effects of the vehicle rocking on its suspension in response to the manipulator's motions are more important than the flexing of the manipulator's links. These large tip errors may exceed the range of simple end-point sensors, such as those used in reference [13], and could result in serious control problems.

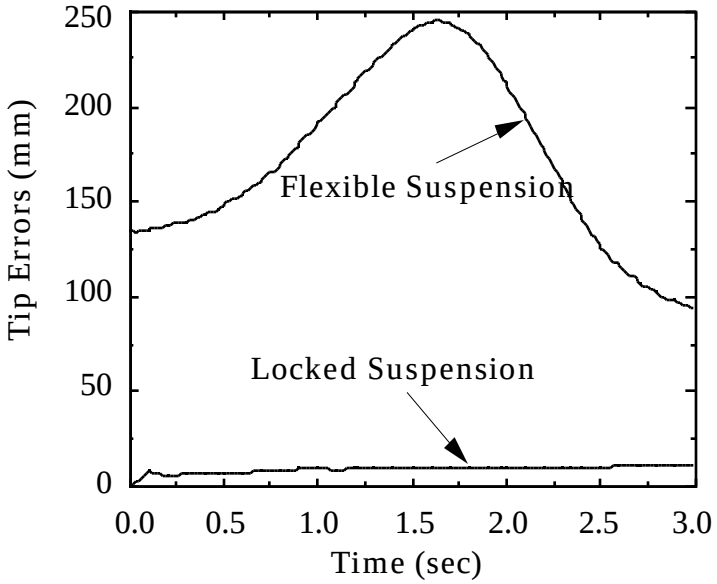

Figure 10. Tip Errors for Flexible Suspension System - Flexible Links

Figure 11 shows the translations and rotations of the vehicle during the motion of the manipulator. The non-zero initial displacements of the vehicle are its static equilibrium position in a gravity field. The rotation of the vehicle about the **Z** axis, ψ_Z, is much smaller than ψ_X and ψ_Y, in the order of 0.014 degrees.

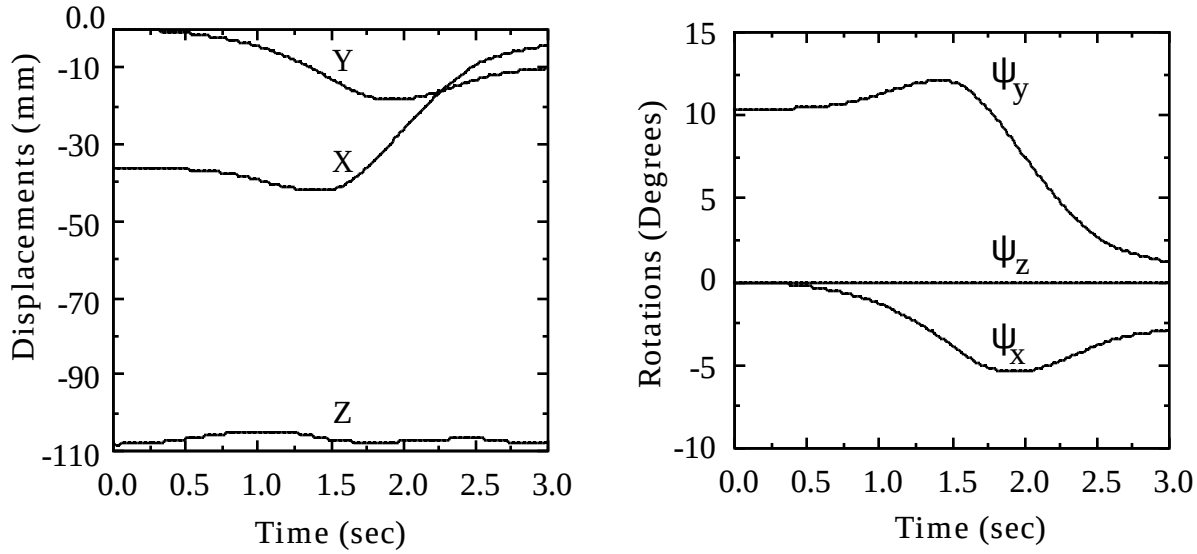

a. Vehicle Translations **b. Vehicle Rotations**

Figure 11. Vehicle Motions

The actuator torques for this simulation are shown in Figure 12. The maximum torque increases to 250 N-m for actuator 1, compared with 150 N-m for the rigid link, locked suspension; and to 1200 N-m for actuator 2, compared with 900 N-m for the rigid link, locked suspension case. Actuator 3 maximum torque remains essentially the same. The increased torques for actuator 1 and actuator 2, due to vehicle tipping, could result in actutator saturation if not accounted for in the system design.

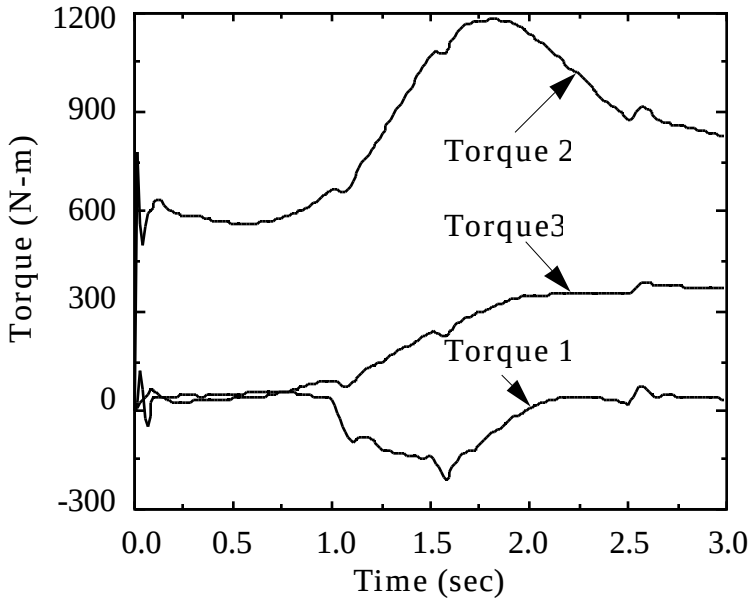

Figure 12. Joint Torques - Flexible links with Flexible Suspension

V. CONCLUSIONS

This paper presents a method for the dynamic analysis of mobile manipulators with link, vehicle and suspension flexibility. It shows that the dynamic interactions between a mobile manipulator and its vehicle can be very important. These interactions can result in large end-effector errors which may exceed the ranges of practical end-point sensing devices. The effects of the dynamic interactions may also saturate the manipulator's actuators. Simple gravity compensators based on rigid link, rigid suspension models may not effectively reduce these errors.

VI. ACKNOWLEDGMENTS

The support of this work by NASA (Langely Research Center Automation Branch) and DARPA (US Army Human Engineering Laboratory and the Oak Ridge National Laboratory as agents) is acknowledged.

VII. REFERENCES

[1] Bronez, M. A., Clarke, M. M., and Quinn, A., "Requirements Development for a Free-Flying Robot - The ROBIN," Proceedings, IEEE International Conference in Robotics and Automation, San Francisco, CA, 1986.

[2] Benner, J., Till, W., and Walz, C., "Automation of Remote Maintenance by an Industrial Robot Mounted on a Gantry Crane," The Proceedings of the Robots and Remote Systems Topical Meeting, Charleston, SC, March 1989.

[3] Blume, C., Gremminger, K., Messemer, G., Smidt, D., and Wadle, M., "EMIR - A Combination Of Manipulator and Robot for New Out-Door Applications in Unstructured Environments," Proc. of the 1989 IEEE Int. Conference on Robotics and Automation, Scottsdale, AZ, pp. 383-390, May 1989.

[4] Dubowsky, S., and Tanner, A. B., "A Study of the Dynamics and Control of Mobile Manipulators Subjected to Vehicle Disturbances," Proc. IV Int. Symp. of Robotics Research, Santa Cruz, CA, 1987.

[5] Sunada, W., and Dubowsky, S., "On the Dynamic Analysis and Behavior of Industrial Robotic Manipulators with Elastic Members," ASME Journal of Mechanisms, Transmissions, and Automation in Design, Vol. 105, pp. 42-51, 1983.

[6] Dubowsky, S., Deck, J. F., and Costello, H., "The Dynamic Modeling of Flexible Spatial Machine System with Clearance Connections," ASME Journal of Mechanisms, Transmissions, and Automation in Design, Vol. 109, pp. 87-94, 1987.

[7] Usuro, P. B., Nadira, R., and Mahil, S. S., ''A Finite Element/Lagrange Approach to Modeling Lightweight Flexible Manipulators,'' ASME Journal of Dynamic Systems, Measurements, and Control, Vol. 108, pp. 198-205, 1986.

[8] Streit, D. A., Krousgrill, C. M., and Bajaj, A. K., "Nonlinear Response of Flexible Robotic Manipulators Performing Repetitive Tasks," ASME Journal of Dynamic Systems, Measurement, and Control, Vol. 111, pp. 471-480, 1989.

[9] Bricout, J. N., Debus, J. C., and Micheau, D., ''A Finite Element Model for the Dynamics of Flexible Manipulators,'' Mechanism and Machine Theory, Vol. 25, No. 1, pp. 119-125, 1990.

[10] Singh, S. N., and Schy, A. A., ''Control of Elastic Robotic Systems by Nonlinear Inversion and Modal Damping,'' ASME Journal of Dynamic Systems, Measurements, and Control, Vol. 108, pp. 180-189, 1986.

[11] Dubowsky, S., and Vance, E. E., "Planning Mobile Manipulator Motions Considering Vehicle Dynamic Stability Constraints," Proceedings of the 1989 IEEE International Conference on Robotics and Automation, Scottsdale, AZ, May 14-19, 1989.

[12] Rakhmanov, Y. V., Strelkov, A. N., and Shvedov, V. N. "Development of a Mathematical Model of a Flexible Manipulator Mounted on a Moving Platform," Engineering Cybernetics, Vol. 19, No. 4, pp. 81-86, 1981.

[13] West, H., Hootsmans, N., Dubowsky, S., and Stelman, N., "Experimental Simulation of Manipulator Base Compliance," Proceedings of the First International Symposium on Experimental Robotics, Montreal, June 19-21, 1989.

[14] Kakizaki, T., Deck, J. F., and Dubowsky, S., "Modeling the Spatial Dynamics of Robotic Manipulators with Flexible Links and Joint Clearances," Proceedings of the 1990 ASME Mechanism Conference, Chicago, IL, Vol. 23-2, pp. 343-350, September 16-19, 1990.